Cancer Management and Research

Dovepress

open access to scientific and medical research

Open Access Full Text Article

ORIGINAL RESEARCH

Long Non-Coding RNA GAS5 Suppresses Tumor Progression and Enhances the Radiosensitivity of Prostate Cancer Through the miR-320a/RAB21 Axis

This article was published in the following Dove Press journal:
Cancer Management and Research

Xiulong Ma[1]
Zhongwei Wang[1]
Hongtao Ren[1]
Xing Bao[1]
Yang Zhang[1]
Baofeng Wang[1]
Dongli Ruan[2]

[1]Department of Radiation Oncology, The Second Affiliated Hospital of Xi'an Jiaotong University, Xi'an, People's Republic of China; [2]Department of Urology, Xijing Hospital, Air Force Military Medical University, Xi'an, Shaanxi 710032, People's Republic of China

Background: Long non-coding RNAs (lncRNAs) function as a class of significant mediators in prostate cancer (PCa), and this study mainly discussed the molecular mechanism of lncRNA growth arrest-specific 5 (GAS5) in PCa progression and radiosensitivity.

Materials and Methods: GAS5 and microRNA-320a (miR-320a) levels were determined by quantitative real-time polymerase chain reaction (qRT-PCR). Cell viability and migration were severally examined through 3-(4, 5-dimethylthiazol-2-y1)-2, 5-diphenyl tetrazolium bromide (MTT) and transwell assays. PCa cells were treated with X-ray irradiation. Cell survival and apoptosis rate were assayed using colony formation assay and flow cytometry, respectively. The apoptosis-related protein and Rab GTPase 21 (*RAB21*) protein levels were measured by Western blot. The relation between miR-320a and GAS5 or *RAB21* was assessed via the dual-luciferase reporter assay. The effect of GAS5 on radiosensitivity of PCa in vivo was evaluated by xenotransplantation assay.

Results: GAS5 was down-regulated in PCa tissues and cells. GAS5 overexpression suppressed cell viability and migration while facilitated radiosensitivity of PCa cells. GAS5 was a molecular sponge of miR-320a. The effects of GAS5 up-regulation on PCa cells were accomplished by sponging miR-320a. MiR-320a targeted *RAB21* and GAS5 up-regulated *RAB21* expression via targeting miR-320a. *RAB21* knockdown reversed the effects of miR-320a inhibition on PCa cells. GAS5 promoted the radiosensitivity of PCa by the miR-320a/*RAB21* axis in vivo.

Conclusion: Collectively, GAS5 restrained tumor development and expedited the radiosensitivity in PCa by the miR-320a/*RAB21* axis, which provided a molecular regulatory mechanism of GAS5/miR-320a/*RAB21* in PCa development and radioresistance.

Keywords: GAS5, prostate cancer, radiosensitivity, miR-320a, *RAB21*

Introduction

Prostate cancer (PCa) is ranked as the second most prevailing cancer and the fifth leading cause of cancer-associated death among males worldwide according to the cancer statistics in 2018.[1] Radiotherapy can prolong the control duration of cancer as a frequently adjunctive therapy of surgical surgery and chemotherapy in PCa treatments.[2,3] The appearance of radioresistance severely limits the therapeutic efficacy of radiotherapy, having detrimental influence on the treatment and prognosis of PCa patients.[4] It is essential to enhance the radiosensitivity in PCa to develop the optional selective treatment of PCa.

Long non-coding RNAs (lncRNAs), without the ability of coding protein, are widely involved in the regulation of various biological behaviors of human cancers

Correspondence: Dongli Ruan
Tel +86-29-84775507
Email gklrhq@163.com

submit your manuscript | www.dovepress.com
DovePress
http://doi.org/10.2147/CMAR.S244123

as the oncogenes or tumor inhibitors.[5,6] Regarding to PCa, lncRNA SOCS2-AS1 was shown to expedite cell growth and refrain apoptosis in PCa cells;[7] UCA1 down-regulation motivated the radiosensitivity and retarded cell progression in PCa via the Akt signaling;[8] Chen et al reported that HULC knockdown contributed to the susceptibility of PCa cells to irradiation through inducing autophagy.[9] Growth arrest-specific 5 (GAS5) is preliminarily defined as a tumor inhibitor in many human cancers,[10] and its down-regulation was found in PCa.[11] GAS5 could inhibit PCa development by targeting miR-145 and regulate radiosensitivity via the inhibition of miR-18a in PCa.[12,13] Nevertheless, the novel molecular mechanism of GAS5 in PCa progression and radiosensitivity remains to be explored.

MicroRNAs (miRNAs) that are a group of short ncRNAs acting as crucial mediators in the cancer process and evolvement by targeting the 3′-untranslated regions (UTR) of messenger RNA (mRNA).[14,15] A set of miRNAs (miR-32-5p, miR-329-3p, miR-127-3p, etc.) was identified as diagnostic biomarkers of PCa due to their dysregulation.[16] Duan et al have discovered that miR-498 expedited cell proliferation, migration, and invasion while lessened radiosensitivity of PCa cells through targeting *PTEN*.[17] Wang et al showed that miR-16-5p promoted the sensitization of PCa cells to radiation by regulating the *Cyclin D1*/E1-pRb-E2F1 pathway.[18] MiR-320a was abnormally up-regulated in PCa cells,[19] but more researches about the biological role of miR-320a on PCa progression and radiosensitivity are needed.

Rab GTPase 21 (*RAB21*) is a subunit of RAB family, in which the members can be the targets of numerous miRNAs. For instance, miR-200b targeted RAB family (*RAB21*, *RAB23*, *RAB18* and *RAB3B*) to be a potential biomarker of breast cancer.[20] In addition, the knockdown of *RAB21* could restrain cell proliferation and trigger apoptosis of glioma cells.[21] A previous study has reported the low expression of RAB21 in PCa tissues,[22] and we then made a speculation that *RAB21* might participate in the regulation of PCa.

Emphatically, this report will investigate the regulatory relationship among GAS5, miR-320a and *RAB21* in the development and radiosensitivity of PCa through the experiments in vitro and in vivo.

Materials and Methods

Tissues Specimens and Cell Culture

Under approval from the Institute Review Ethics Committee of The Second Affiliated Hospital, School of Medicine, 51 pairs of tissues (including PCa tissues and normal paracancerous tissues) were collected from 51 PCa patients at The Second Affiliated Hospital, School of Medicine. These PCa specimens were divided into I+II stages (n=21) and III+IV stages (n=30) following the tumor stage by the American Joint Committee on Cancer criteria (AJCC).[23] Before the prostatectomy, all patients were fully informed concerning our research purpose and signed the written informed consent form. These tissue samples were conserved in liquid nitrogen.

The source of all cell lines was COBIOER (Nanjing, China), containing human PCa cell lines (DU145 and LNCaP) and normal prostate stroma cell line WPMY-1. Our purchase of cell lines was performed after obtaining the authorization from the Institutional review committee of The Second Affiliated Hospital, School of Medicine. Cell culture was implemented in a 37°C, 5% CO_2 incubator using basic Roswell Park Memorial Institute-1640 (RPMI-1640; Gibco, Carlsbad, CA, USA) supplemented with 10% fetal bovine serum (FBS; Gibco) and 1% penicillin-streptomycin antibiotic solution (Gibco).

Vectors or Oligonucleotides Transfection

The sequence of GAS5 was amplified and inserted into a mammalian expression vector pcDNA3.1 (Invitrogen, Carlsbad, CA, USA) to construct the recombinant vector pcDNA3.1-GAS5 (GAS5). MiR-320a/negative control (NC) mimic (miR-320a and miR-NC), miR-320a/NC inhibitor (anti-miR-320a and anti-NC), small interfering RNA (siRNA) against GAS5/NC (si-GAS5 and si-NC) were all bought from GenePharma (Shanghai, China). When DU145 and LNCaP cells were grown to 60% coverage, cell transfection was administered using the Lipofectamine3000 (Invitrogen) following the manufacture's operating protocol.

Quantitative Real-Time Polymerase Chain Reaction (qRT-PCR)

The QuantiFast SYBR® Green PCR Kit (Qiagen, Hilden, Germany) was used for performing the qRT-PCR reaction using complementary DNA (cDNA) as amplified template, which was synthesized by QuantiTect Reverse Transcription Kit (Qiagen) after the isolation of total RNA from tissues or cells by Trizol (Beyotime, Shanghai, China). The fold-changes of GAS5 and miR-320a were analyzed by $2^{-\Delta\Delta Ct}$ method by the respective comparison with glyceraldehyde-3-phosphate dehydrogenase (GAPDH) and U6.[24] The primers were listed as below: GAS5: 5′-AACTT

GCCTGGACCAGCTTA-3′ (forward) and 5′-CAAGCCGA CTCTCCATACCT-3′ (reverse); miR-320a: 5′-GGGCTAA AAGCTGGGTTGA-3′ (forward) and 5′-CAGTGCGTG TCGTGGAGT-3′ (reverse); *GAPDH*: 5′-ACCTGACCTGC CGTCTAGAA-3′ (forward) and 5′-TCCACCACCCTG TTGCTGTA-3′ (reverse); U6: 5′-CGCTTCGGCAGCAC ATATACTAAAATTGGAAC-3′ (forward) and 5′-GCTTCA CGAATTTGCGTGTCATCCTTGC-3′ (reverse).

3-(4, 5-Dimethylthiazol-2-y1)-2, 5-Diphenyl Tetrazolium Bromide (MTT) Assay

DU145 and LNCaP cells in the logarithmic phase were severally plated into the 96-well plates (Corning Inc., Corning, NY, USA) overnight. Following cell transfection 0 h, 24 h, 48 h and 72 h, MTT (Invitrogen) was pipetted into the wells of plates with 20 μL per well for 4 h. Then cells were added with 200 μL dimethyl sulfoxide (DMSO; Beyotime) after cell supernatants were removed. At 10 min post-incubation, the absorbance (at the wavelength of 490 nm) was recorded under a microplate reader (Thermo Fisher Scientific, Waltham, MA, USA).

Transwell Migration Assay

The upper chamber of transwell 24-well chamber (Corning Inc.) was seeded with 5×10^3 cells in serum-free RPMI-1640 medium, and the medium containing 10% FBS was added into the lower chamber in the meantime. Twenty-four-hour later, the unmigrated cells were erased by a sterile wet swab, then the migrated cells passed the membranes were fastened in 4% paraformaldehyde and dyed using crystal violet (Sangon, Shanghai, China), followed by the photographing through a microscope with the magnification of 100 × and the number of migrated cells was counted.

X-Ray Irradiation Treatment

After cells were inoculated into the 24-well-plates overnight and transfected with different groups for 24 h, X-ray irradiation were treated to PCa cells with the different doses (0, 2, 4, 6, and 8 Gy) through a linear accelerator (Siemens, Princeton, NJ, USA) with the 6-MeVX photo beam at the dose rate of 2 Gy/min.

Colony Formation Assay

Harvested cells were transplanted into the 6-well plates at a plating density of 200 cells/well. Incubating for 14 d, the formative colonies were fixed with methanol and stained with crystal violet (Sangon). The colonies (over 50 cells as a colony) were photographed by a camera and the survival fraction was calculated according to the formula: the colonies number/(inoculated cells number × plating efficiency).

Flow Cytometry

The apoptotic cells were assayed by Annexin V-fluorescein isothiocyanate (Annexin V-FITC)/propidium iodide (PI) kit (Sigma, St. Louis, MO, USA). The digested cells were centrifugally (3000 rpm/min for 15 min) collected and washed with pre-cooled 1 × phosphate buffered saline (PBS; Corning Inc.), followed by the cell resuspension in 500 μL 1 × binding buffer. Then cell suspension was stained in line with the operating protocol of the provider. The labeled apoptotic cells (Annexin V+/PI- and Annexin V+/PI+) could be distinguished on the flow cytometer (BD Biosciences, San Diego, CA, USA) and the apoptosis rate (apoptotic cells/total cells ×100%) was calculated finally.

Western Blot Assay

The protein extraction was executed by Radio Immunoprecipitation Assay (RIPA) lysis buffer (Sangon). After the quantification by a BCA Protein Assay Kit (Takara, Beijing, China), 40 μg proteins were mixed with sodium dodecyl sulfate polyacrylamide gel electrophoresis (SDS-PAGE) loading buffer (Takara) and separated by SDS-PAGE (Voltage: 120V, electric current: 60 mA) for 2 h. The protein transferring was performed through polyvinylidene fluoride membranes (Sangon) and non-specific protein-binding blockage was conducted in 5% non-fat milk (Sangon) for 3 h. Afterwards, the membranes were incubated with primary antibodies from Abcam (Cambridge, UK) including anti-Cleaved-caspase3 (anti-C-casp3; ab32042, 1:1000), anti-Cleaved-caspase9 (anti-C-casp9; ab2324, 1:1000), anti-*RAB21* (ab224390, 1:1000) and internal control anti-*GAPDH* (ab181602, 1:3000) for 5 h at indoor temperature. The secondary antibody (Abcam, ab205718, 1:5000) was conjugated with primary antibodies for 1 h, followed by the detection of blots through the enhanced chemiluminescence reagent (Beyotime). Ultimately, the protein bands were imaged by ImageLab software version 4.1 (Bio-Rad Laboratories, Hercules, CA, USA) and the densitometry was analyzed as previously described.[25]

Dual-Luciferase Reporter Assay

In the beginning, the luciferase reporters were constructed through molecular cloning, including wild-type and mutant-type GAS5 (GAS5 WT and GAS5 MUT) as well as wild-type and mutant-type *RAB21* 3′UTR (RAB21-WT and RAB21-MUT). The wild-types contained the sites of miR-320a and mutant-types indicated that the miR-320a binding sites in wild-types were mutated. After co-transfection of these above reporters and miR-320a or miR-NC for 48 h, the luciferase intensity of PCa cell lysates in the passive buffer (Promega, Madison, WI, USA) was measured by the dual-luciferase reporter system (Promega) complying with the manufacturer's instruction. The renilla acted as the normalized control for firefly luciferase and the ratio of firefly/renilla luciferase intensity represented the relative luciferase activity.

Xenotransplantation Assay

The purchased 5-week-old BALB/c nude mice (Vital River Laboratory Animal Technology, Beijing, China) were fed in specific pathogen-free cage (temperature at 18–23°C, humidness at 50–60%, and 12 h day/night cycle), and the food and water were carefully disinfected to provide for all mice. After 1 week, xenotransplantation model was constructed by subcutaneously injecting 100 μL DU145 cell suspension in PBS (1×10^6 cells) stably expressed GAS5 or vector into the back of mice with 10 mice/group. Then half mice were respectively exposed to 4 Gy X-ray irradiation every other day for 3 days, hence all mice were divided into four groups vector, GAS5, vector+4 Gy and GAS5+4 Gy (5 mice per group). Tumors were monitored by digital calipers and tumor volume was weekly estimated using the formula: (length × width^2) × 0.5.[26] Five weeks later, tumor weight was measured after tumors were excised from mice sacrificed by displacing 60% air of cage volume using the flow rate of CO_2 per min in compliance with the current guideline of the American Veterinary Medical Association (AVMA). Following the extraction of total RNA and protein from tumor tissues, the qRT-PCR (for GAS5 and miR-320a) and Western blot (for *RAB21*) were conducted for the expression analyses of three molecules. This assay was strictly in accordance with the Guide to the Management and Use of Laboratory Animals issued by the National Institutes of Health, and all operating protocols were ratified by the Animal Ethics Committee of The Second Affiliated Hospital, School of Medicine.

Statistical Analysis

All data were presented as the mean ± standard deviation (SD) based on three independent repetitions with N=3 per time, and the statistical analysis was performed by SPSS 20.0. The difference comparison relied on Student's *t*-test and one-way analysis of variance (ANOVA) followed by Tukey's test. $P < 0.05$ was regarded as a significant difference. The graphics rendering was carried out using GraphPad Prism 7.

Results

The Down-Regulation of GAS5 Was Prominent in PCa Tissues and Cells

The dysregulation of GAS5 in PCa was notarized by qRT-PCR firstly. Making a comparison to normal non-cancerous tissues, GAS5 expression was aberrantly reduced in PCa tissues (Figure 1A). And noticeably, the level of GAS5 in III+IV stage tissues (n=30) was considerably lower than that in I+II stage tissues (n=21) (Figure 1B). This low expression of GAS5 was also shown in DU145 and LNCaP cells relative to the normal WPMY-1 cells (Figure 1C). Positively, GAS5 was down-regulated in PCa tissues and cells, which might be relevant to the cancer development in PCa.

Up-Regulation of GAS5 Suppressed PCa Cell Viability and Migration

We constructed the overexpression vector GAS5 to explore the biological function of GAS5 in PCa. After transfection of GAS5 in DU145 and LNCaP cells, qRT-PCR exhibited its satisfactory overexpression effect on GAS5 level, compared to the vector transfection group (Figure 2A and B). Following the MTT assay, DU145 (Figure 2C) and LNCaP (Figure 2D) cells manifested the lower cell viability as a result of GAS5 overexpression. Similarly, the migrated DU145 cells of GAS5 transfection group were overtly decreased by contrast to the vector group (Figure 2E), and the same phenomenon was observed in LNCaP cells (Figure 2F). Summarily, the increase of GAS5 expression brought about the inhibition of PCa cell viability and migration.

GAS5 Overexpression Contributed to Radiosensitivity in PCa Cells

At 24 h post-transfection of GAS5 or vector, DU145 and LNCaP cells were treated with X-ray irradiation (0–8 Gy) to induce cell damage, then the effect of GAS5 on

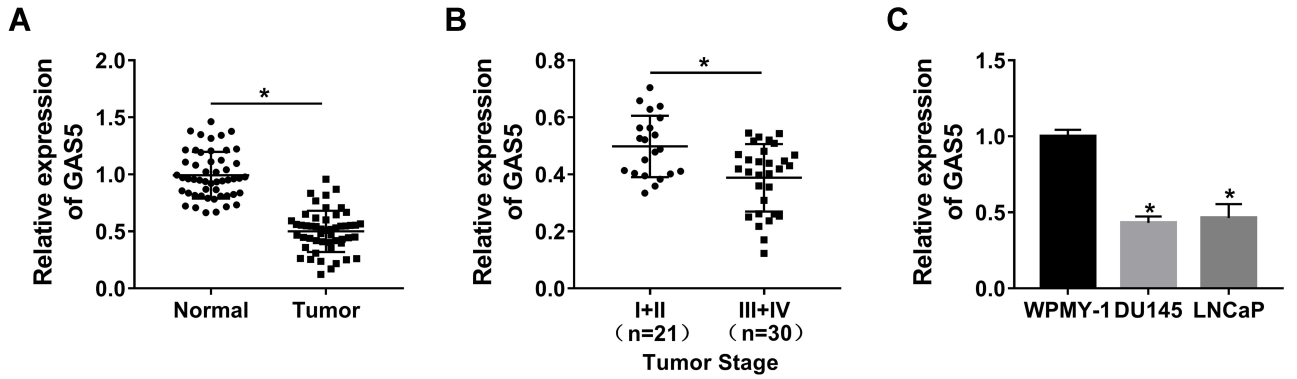

Figure 1 The down-regulation of GAS5 was prominent in PCa tissues and cells. (**A–C**) GAS5 expression was assayed by qRT-PCR in PCa tissues (**A**), I+II and III+IV staged tissues (**B**), as well as in DU145 and LNCaP cells (**C**). *$P < 0.05$.

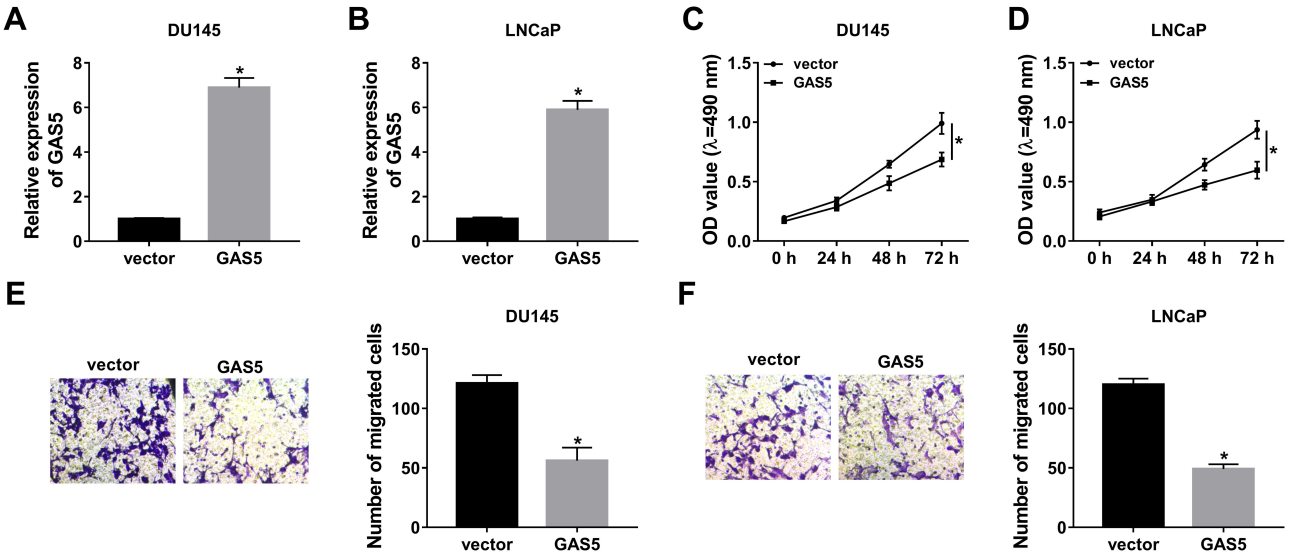

Figure 2 Up-regulation of GAS5 suppressed PCa cell viability and migration. GAS5 or vector was transfected into DU145 and LNCaP cells. (**A, B**) The transfection efficiency of GAS5 was evaluated by qRT-PCR. (**C, D**) Cell viability was assayed through MTT. (**E, F**) Cell migration was detected using transwell assay. *$P < 0.05$.

radiosensitivity was investigated via the analyses of cellular processes. Colony formation assay revealed that the promotion of GAS5 led to the apparent decline of survival fraction after X-ray radiation (2–8 Gy) (Figure 3A and B). As regards cell apoptosis, we found that the apoptosis rate had no obvious change in GAS5 and vector groups without X-ray irradiation, but the introduction of GAS5 remarkably enhanced the apoptosis rate in DU145 (Figure 3C) and LNCaP (Figure 3D) cells treated with 4 Gy of X-ray irradiation. The detection of C-casp3 and C-casp9 (pro-apoptosis markers) verified this point again. Western blot indicated that both C-casp3 and C-casp9 protein levels were strikingly heightened after the high expression of GAS5 when DU145 (Figure 3E) and LNCaP (Figure 3F) cells were exposed to 4 Gy radiation. All the data proved the stimulative effect of GAS5 on radiosensitivity in PCa cells.

GAS5 Acted as the Molecular Sponge of miR-320a

Subsequently, the binding sites between GAS5 and miR-320a (CAGCUUU-GUCGAAA) were predicted by Starbase 3.0 software (Figure 4A). The dual-luciferase reporter assay demonstrated that the normalized luciferase activities of DU145 and LNCaP cells were dramatically decreased following GAS5 WT and miR-320a co-transfection, but GAS5 MUT and miR-320a co-transfection made no marked difference of luciferase activity, compared to the GAS5 WT +miR-NC or GAS5 MUT+miR-NC group (Figure 4B). QRT-PCR presented the memorable up-regulation of miR-320a in PCa tissues (Figure 4C) and cells (DU145 and LNCaP) (Figure 4D) by comparison with the normal tissues and WPMY-1 cells. In addition, GAS5 overexpression

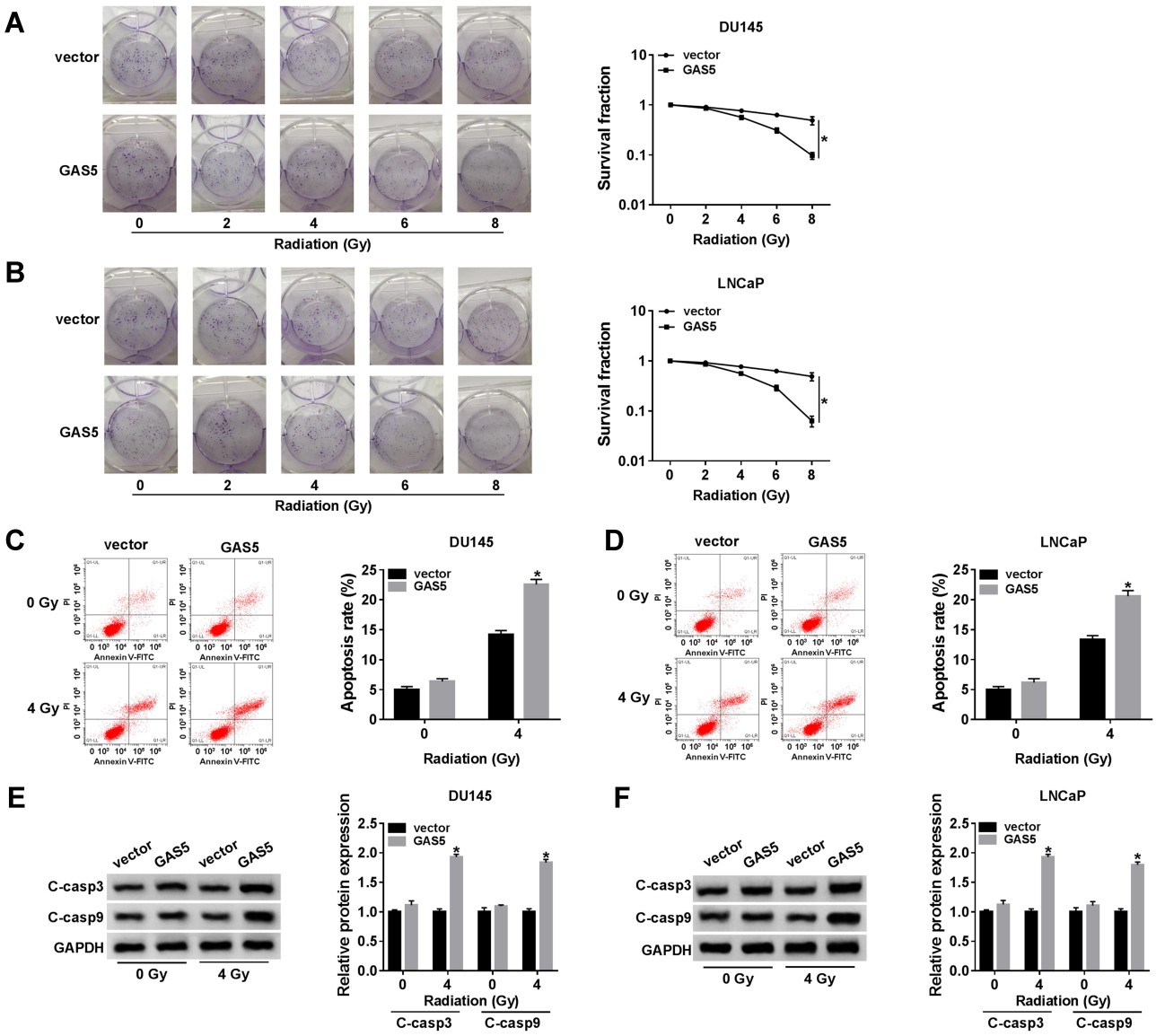

Figure 3 GAS5 overexpression contributed to radiosensitivity in PCa cells. DU145 and LNCaP cells were transfected with GAS5 or vector for 24 h. (**A, B**) Cell survival was examined by colony formation assay after 0–8 Gy radiation. (**C, F**) Cell apoptosis was assessed through the apoptosis rate by flow cytometry (**C, D**) and the detection of apoptosis markers by Western blot (**E, F**) following 0 Gy radiation (without radiation) and 4 Gy radiation. *$P < 0.05$.

triggered the down-regulation of miR-320a expression in DU145 (Figure 4E) and LNCaP (Figure 4F) cells. These outcomes clarified that miR-320a was a target of GAS5 and GAS5 acted as a nature sponge of miR-320a.

GAS5 Regulated Cell Viability, Migration and Radiosensitivity of PCa Cells by Sponging miR-320a

Through the analysis of qRT-PCR, the miR-320a level of miR-320a transfection group was significantly higher than that of miR-NC group in DU145 and LNCaP cells, implying that miR-320a was successfully overexpressed via miR-320a mimic (Figure 5A and B). The regulatory effects of GAS5 and miR-320a on PCa cells were investigated by the reverted experiments. As shown in Figure 5C and D, the absorbance of GAS5+miR-320a group was distinctly increased contrasted to GAS5 +miR-NC group in MTT assay. And the GAS5-induced repressive effect on cell migration was rescued after the overexpression of miR-320a in DU145 (Figure 5E) and LNCaP (Figure 5F) cells. Besides, GAS5 transfection aggravated the decline of survival (Figure 5G and H) and the increase of apoptosis rate (Figure 5I and J)

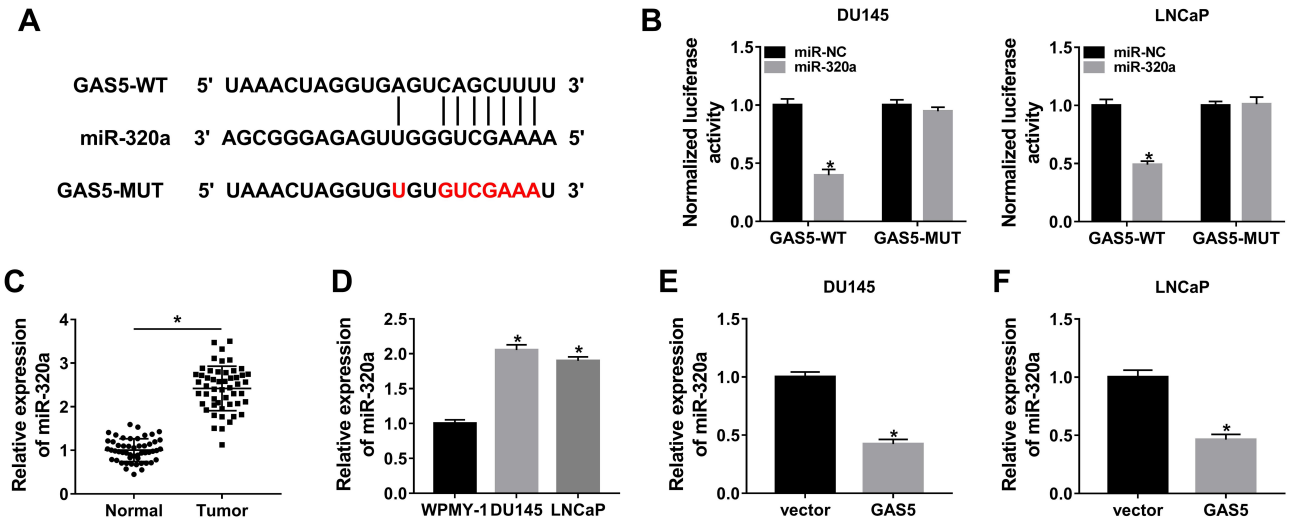

Figure 4 GAS5 acted as the molecular sponge of miR-320a. (**A**) The target sites between GAS5 and miR-320a were predicted using Starbase 3.0. (**B**) The analysis of the combination between GAS5 and miR-320a was conducted by the dual-luciferase reporter assay. (**C, D**) The qRT-PCR was used for the determination of miR-320a expression in PCa tissues and cells. (**E, F**) The level of miR-320a was assayed by qRT-PCR in PCa cells transfected with GAS5 or vector. *$P < 0.05$.

caused by X-ray radiation, whereas miR-320a up-regulation inversed these effects. Similarly, the presence of miR-320a abrogated the GAS5-mediated up-regulation of C-casp3 and C-casp9 protein levels in DU145 (Figure 5K) and LNCaP (Figure 5L) cells subjected to 4 Gy X-ray irradiation. Altogether, the regulation of GAS5 on the evolvement and radiosensitivity of PCa cells was depending on sponging miR-320a.

miR-320a Directly Targeted RAB21 and GAS5 Positively Regulated RAB21 Expression by Targeting miR-320a

The target of miR-320a was searched by Starbase 3.0, in which *RAB21* 3′UTR was found to have the target points to bind to miR-320a in sequences (Figure 6A). We used the dual-luciferase reporter assay to explore whether *RAB21* could combine with miR-320a. In comparison with miR-NC transfection, miR-320a transfection signally inhibited the luciferase activity of RAB21-WT group but not RAB21-MUT group (Figure 6B), suggesting the interaction between miR-320a and *RAB21*. Whereafter, we observed the clear decline of *RAB21* protein expression in PCa tissues compared with normal tissues (Figure 6C), as well as in DU145 and LNCaP cells in contrast to WPMY-1 cells (Figure 6D). Overtly, the *RAB21* protein level was decreased in DU145 (Figure 6E) and LNCaP (Figure 6F) cells because of miR-320a transfection. Furthermore, GAS5 overexpression resulted in increase of *RAB21* protein expression, which was abolished by the enhancement of miR-320a level (Figure 6G and H). Collectively, *RAB21* was a target of miR-320a and GAS5 promoted the level of *RAB21* through sponging miR-320a.

Down-Regulation of RAB21 Reversed the Effects of miR-320a Inhibition on PCa Cells

We used si-RAB21 transfection to knock down *RAB21* in PCa cells, as Figure 7A and B depicted, the knockdown efficiency of si-RAB21 was great in both DU145 and LNCaP cells contrasted to si-NC group. After transfection of anti-miR-320a, anti-miR-320a+si-RAB21 or matched controls, the biological regulation of miR-320a and *RAB21* in PCa cells was researched. MTT and transwell assays exhibited that miR-320a inhibitor notably reduced cell viability (Figure 7C and D) and migration (Figure 7E and F) of DU145 and LNCaP cells, while knockdown of *RAB21* ameliorated these repressive effects. Moreover, the X-ray irradiation-induced cell survival suppression (Figure 7G and H) and apoptosis promotion (Figure 7I and J) were aggravated by the miR-320a inhibitor, whereas these effects were reverted following the *RAB21* down-regulation. Also, transfection of si-RAB21 counteracted the anti-miR-320a-motivated accelerative effects on C-casp3 and C-casp9 protein expression in DU145 (Figure 7K) and LNCaP (Figure 7L) cells treated with 4 Gy irradiation. Above results suggested that the effects of miR-320a repression on reducing cell viability and migration as well as

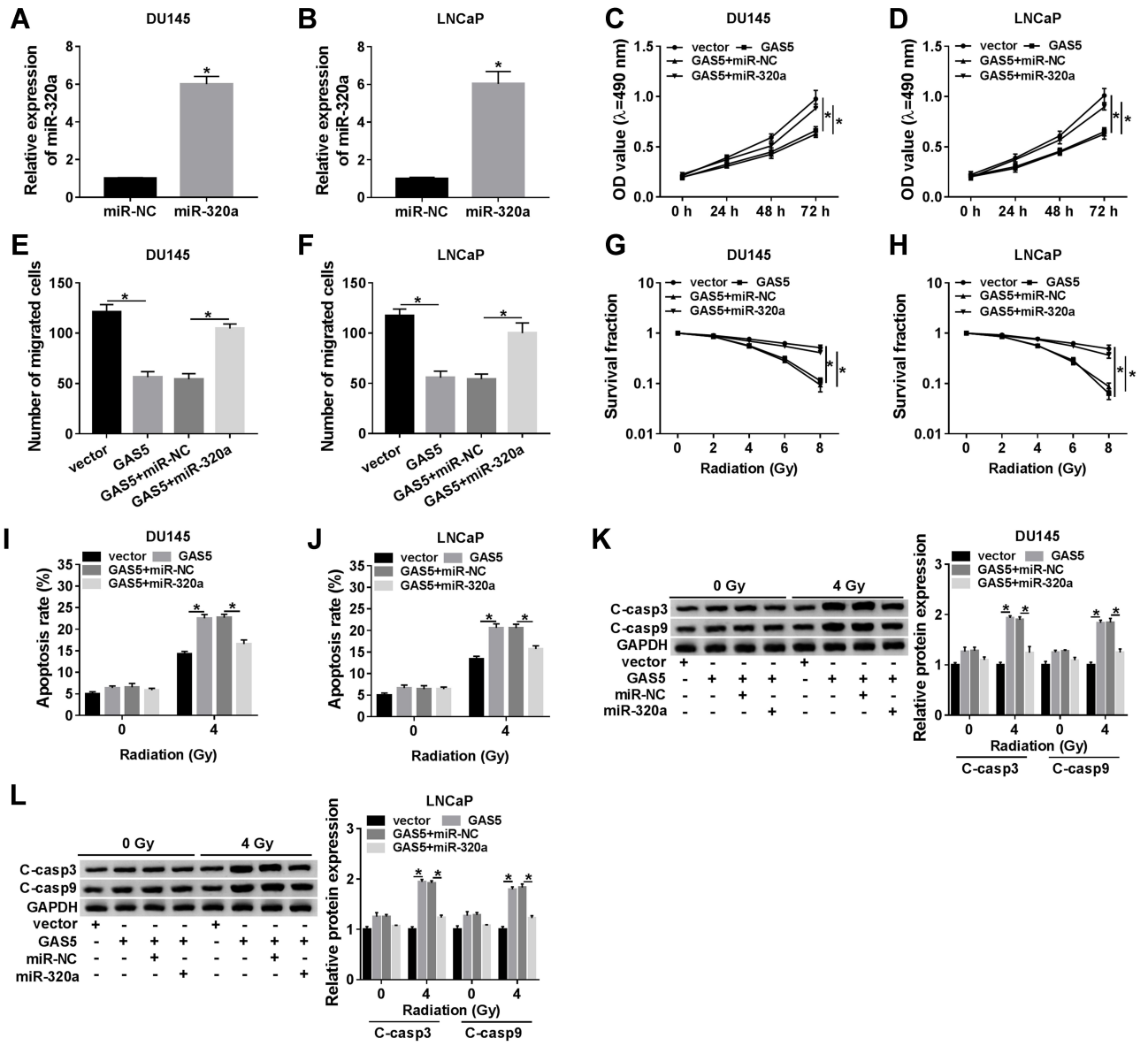

Figure 5 GAS5 regulated cell viability, migration and radiosensitivity of PCa cells by sponging miR-320a. (**A, B**) The transfection efficiency of miR-320a was detected through qRT-PCR. (**C, D**) MTT was applied to analyze cell viability after transfection of vector, GAS5, GAS5+miR-NC or GAS5+miR-320a. (**E, F**) The measurement of cell migration was carried out by transwell assay. (**G, H**) The assessment of cell survival was performed using colony formation assay after transfection and X-ray irradiation. (**I, J**) The apoptosis was determined by flow cytometry. (**K, L**) The protein levels of C-casp3 and C-casp9 were examined by Western blot. *$P < 0.05$.

expediting radiosensitivity were all relieved by the down-regulation of *RAB21* in PCa cells.

GAS5 Inhibited Tumor Growth and Facilitated the Radiosensitivity of PCa via the miR-320a/RAB21 Axis in vivo

We designed the animal experiment by establishing the xenotransplantation model in mice as Fig. 8A, for researching the role of GAS5 in PCa in vivo. GAS5 inhibited tumor volume and weight in established mice model, and accentuated the 4 Gy X-ray irradiation-induced repression of tumor growth (Fig. 8B–C). Besides, the expression of GAS5 was boosted in GAS5 groups (Fig. 8D). Inversely, GAS5 overexpression evoked the down-regulation of miR-320a expression (Fig. 8E). And Western blot demonstrated that RAB21 expression was prominently higher in GAS5 groups than that in the vector groups (Fig. 8F). Shortly, GAS5 reduced tumor growth and enhanced radiosensitivity in PCa by the miR-320a/*RAB21* axis in vivo.

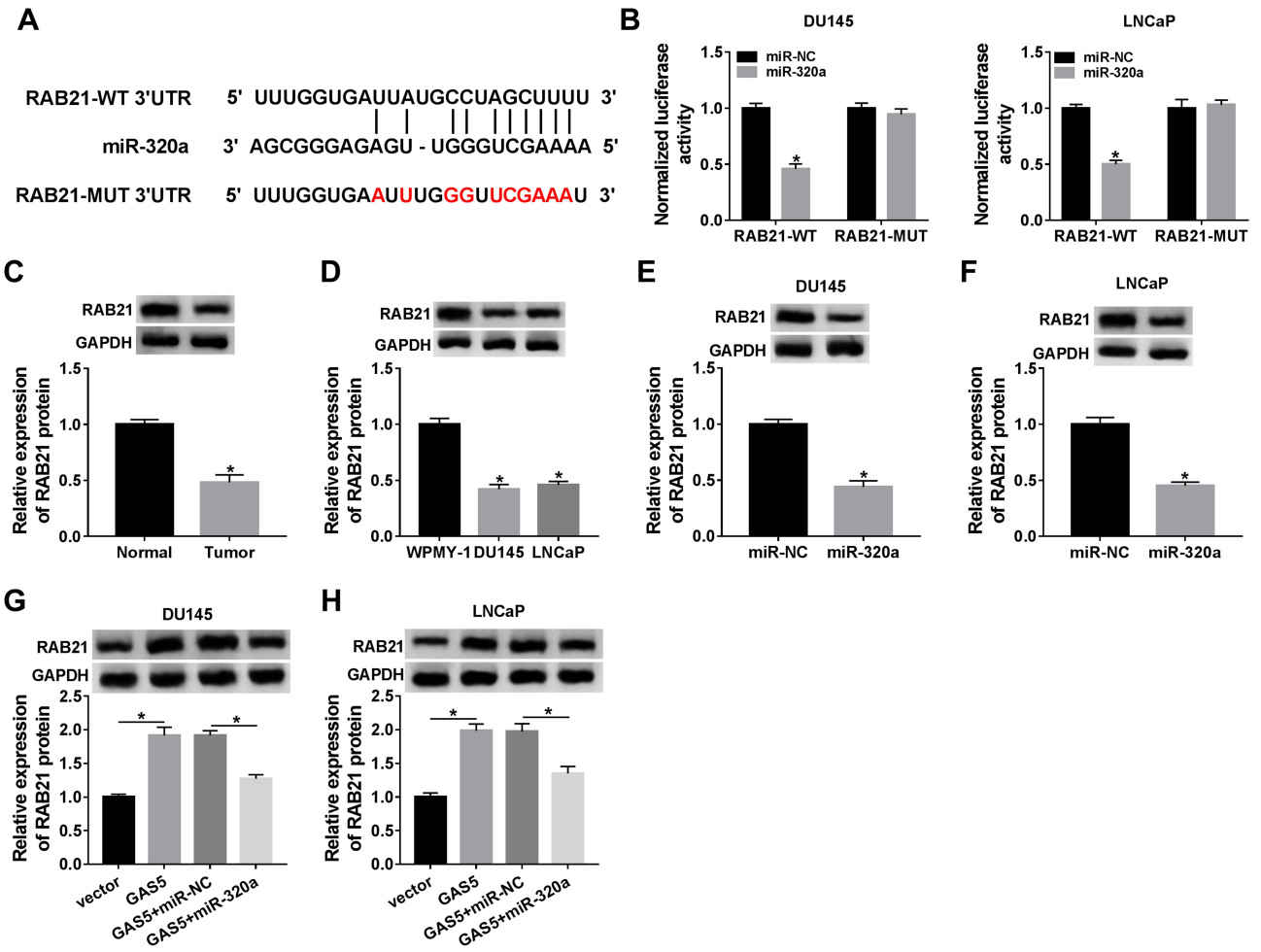

Figure 6 MiR-320a directly targeted *RAB21* and GAS5 positively regulated *RAB21* expression by targeting miR-320a. (**A**) Starbase 3.0 was implemented for the analysis of the binding sites between miR-320a and *RAB21*. (**B**) The interaction relation between miR-320a and *RAB21* was explored via the dual-luciferase reporter assay. (**C, D**) Western blot assay was performed to assay the *RAB21* protein expression in PCa tissues and cells. (**E, F**) The effect of miR-320a mimic on the *RAB21* protein level was analyzed by Western blot. (**G, H**) *RAB21* protein expression was measured by Western blot in DU145 and LNCaP cells transfected with GAS5, GAS5+miR-320a or relative controls. *$P < 0.05$.

Discussion

To our delight, the 5-year survival rate of PCa patients has been increased in many countries all over the world, which benefits from the radiotherapy in part.[27,28] However, searching molecular targets for elevating radiosensitivity becomes increasingly important to overcome the acquired radioresistance.[4,29] Fortunately in our study, lncRNA GAS5 was considered as a candidate biomarker for the radiation treatment of PCa.

Dysregulation of lncRNAs may be responsible for the occurrence of multiple human cancers, including PCa.[30,31] It is worth noting that GAS5 is provably down-regulated in various cancers and has the potential to be a tumor inhibitor.[32–34] With one accord, our results proved the inhibition of GAS5 expression in PCa tissues and cells. Additionally, Wang et al documented that the down-regulation of GAS5 enhanced cell proliferation and doxorubicin resistance of hepatocellular carcinoma through regulating the miR-21/*PTEN* signals.[35] Long et al announced the inhibitory effect of GAS5 on tumor development and stimulation of chemosensitivity of ovarian cancer was attributed to the GAS5-*E2F4*-*PARP1*-*MAPK* axis.[36] And GAS5 overexpression was recorded to increase the radiosensitivity of cervical cancer cells via the regulation of miR-106/*IER3* and non-small cell lung cancer (NSCLC) cells through decreasing the level of miR-135b.[37,38] In conformity with these statements, the impacts of GAS5 on suppressing cell viability, migration and promoting the radiosensitivity of PCa cells were exhibited in our current study.

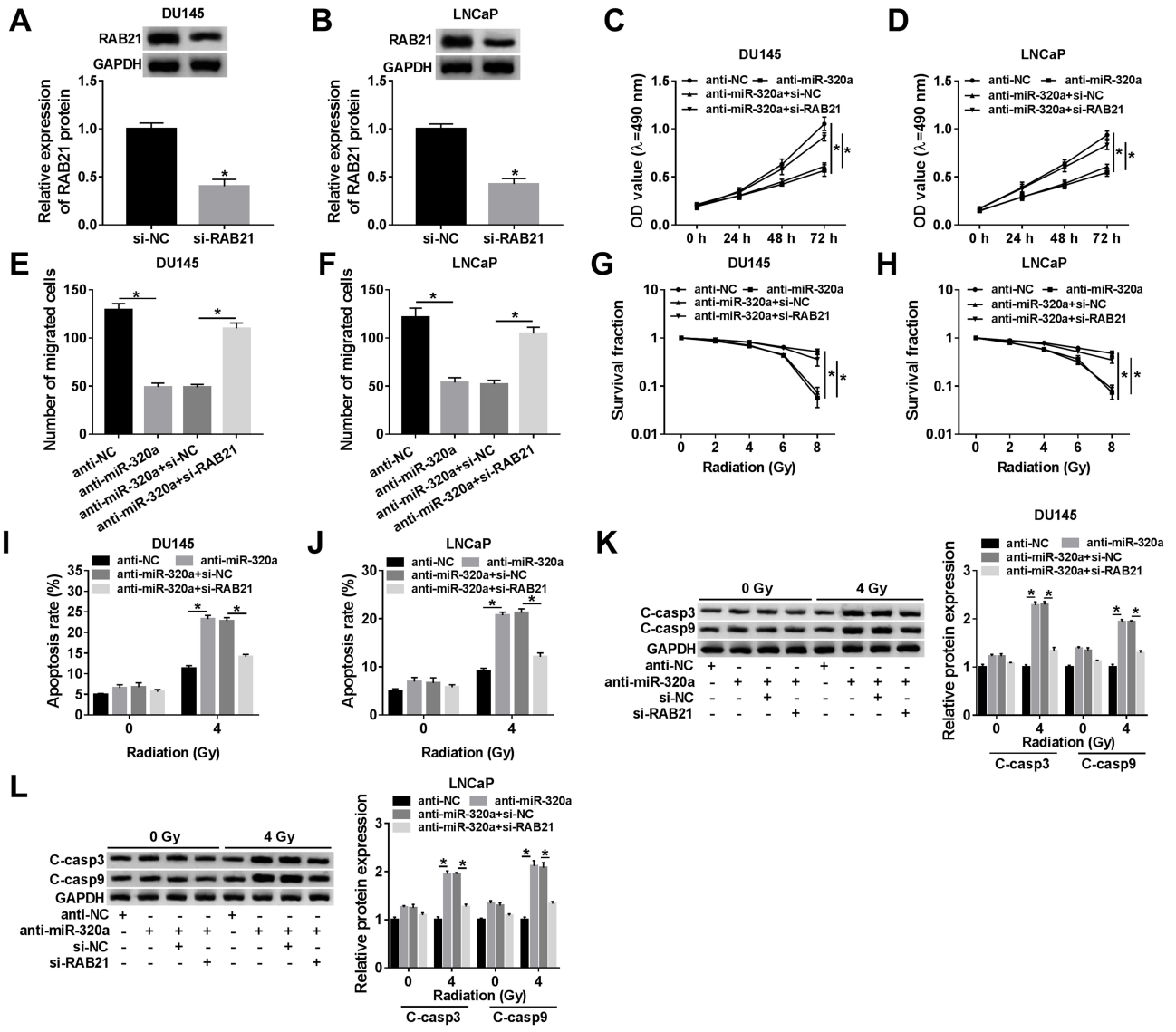

Figure 7 Down-regulation of *RAB21* reversed the effects of miR-320a inhibition on PCa cells. (**A, B**) The interference effect of si-RAB21 on *RAB21* expression was examined via Western blot. (**C, D**) The determination of cell viability was administrated by MTT in anti-miR-320a, anti-miR-320a+si-*RAB21* or respective control groups. (**E, F**) Transwell assay was applied for detecting cell migrated ability. (**G, H**) Colony formation assay was exploited to analyze cell survival after transfection and radiation. (**I–L**) The apoptosis rate by flow cytometry (**I, J**) and the assaying of apoptosis-related proteins via Western blot (**K, L**) were used for assessing cell apoptosis. *$P < 0.05$.

The roles of lncRNAs commonly depend on acting as the sponges of miRNAs in cancers.[39,40] We clarified that GAS5 directly targeted miR-320a and restrained the miR-320a level. Researches of miR-320a presented the high expression of it in several cancers and the involvement in tumor regulation. For example, miR-320a was up-regulated and repressed cell proliferation, metastasis in NSCLC by PI3K/AKT signaling pathway.[41] And miR-320a was highly expressed in neuroblastoma cells and inhibited the sensitivity of pancreatic cancer cells to 5-FU.[42,43] Herein, miR-320a expression was aberrantly increased in PCa tissues and cells. And GAS5 overexpression-induced inhibition of tumor progression and promotion of radiosensitivity in PCa cells were ameliorated by miR-320a, insinuating the oncogenic role of miR-320a in PCa and the effects of GAS5 were attained by sponging miR-320a.

And interestingly, the combination between miRNAs and the 3′UTR of mRNAs endows the regulatory capacity to miRNAs in mammalian cells.[44,45] Through the validation of experiments, *RAB21* was a target of miR-320a and negatively regulated by miR-320a. The down-regulation of *RAB21* in PCa during this study was in accordance with the article earlier.[22] Besides, miR-320a increased cell viability

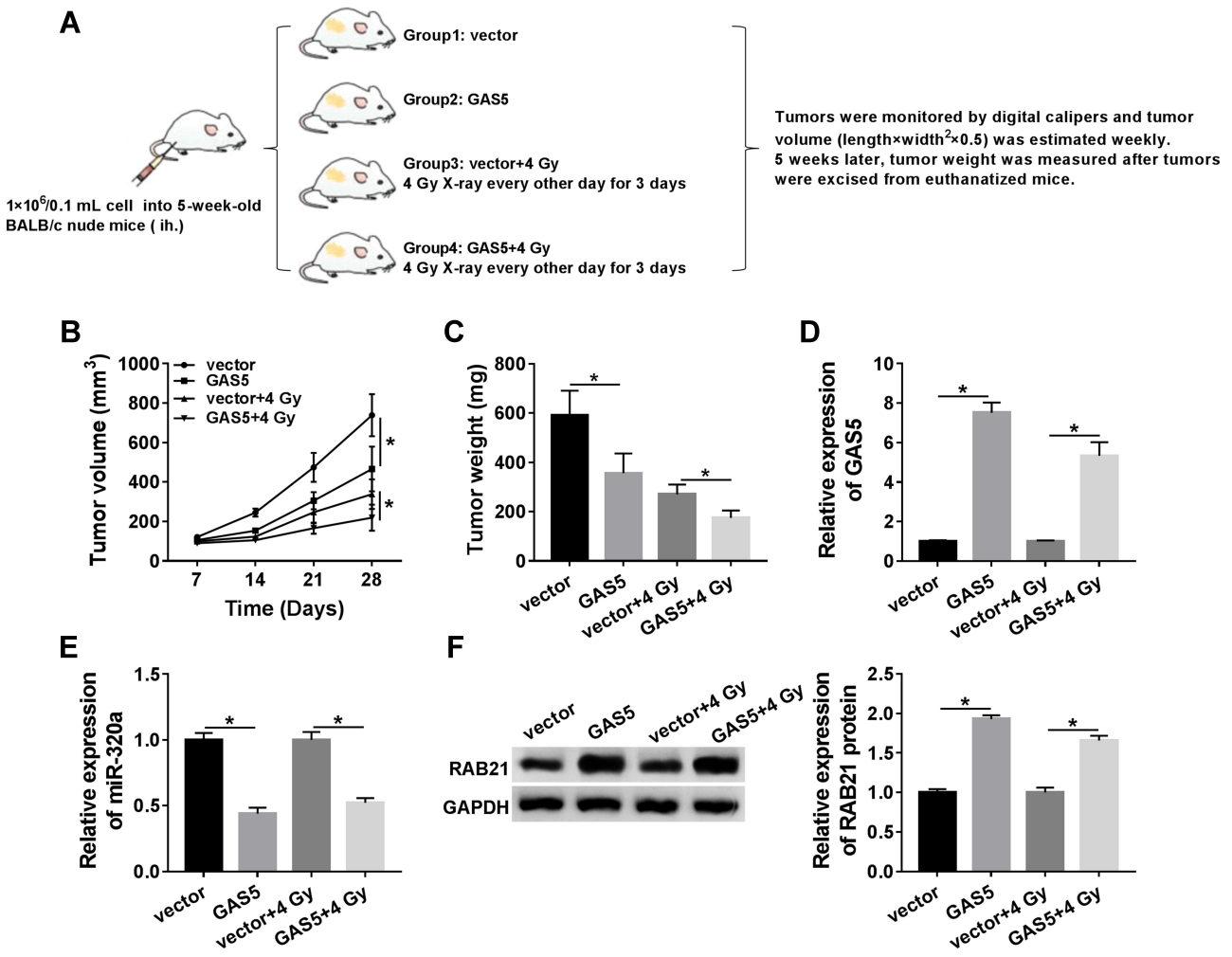

Figure 8 GAS5 inhibited tumor growth and facilitated the radiosensitivity of PCa via the miR-320a/*RAB21* axis in vivo. (**A**) The design figure of this animal experiment. (**B, C**) Tumor volume (**B**) and weight (**C**) were measured in vector, GAS5, vector+4 Gy or GAS5+4 Gy groups. (**D, E**) QRT-PCR was administrated to analyze the expression of GAS5 and miR-320a after RNA extraction from tumor tissues. (**F**) Western blot was used to examine the protein expression of *RAB21* after protein isolation from tumor tissues. *$P < 0.05$.

and migration but inhibited radiosensitivity via repressing *RAB21* expression level in PCa cells. Furthermore, GAS5 acted as a sponge of miR-320a, consequently resulting in the positive regulation of *RAB21* expression. Moreover, the assays in vivo also confirmed that GAS5 decreased tumor growth and motivated the radiosensitivity of PCa by acting on the miR-320a/*RAB21* axis.

Conclusion

To conclude, our study unraveled the molecular mechanism of lncRNA GAS5 in the inhibition of tumor progression and the promotion of radiosensitivity in PCa by the miR-320a/*RAB2*1 axis. The GAS5/miR-320a/*RAB21* regulatory axis may be favorable to enhance the therapeutic effect of radiotherapy, and GAS5 can serve as a positive indicator in the suppression and alleviation of PCa progression.

Abbreviations

PCa, prostate cancer; lncRNAs, long non-coding RNAs; GAS5, growth arrest-specific 5; UTR, untranslated regions; *RAB21*, Rab GTPase 21; NSCLC, non-small cell lung cancer; qRT-PCR, quantitative real-time polymerase chain reaction; RIPA, Radio Immunoprecipitation Assay; SDS-PAGE, sodium dodecyl sulfate polyacrylamide gel electrophoresis; SD, standard deviation.

Data Sharing Statement

The analyzed data sets generated during the present study are available from the corresponding author on reasonable request.

Ethics Approval and Consent to Participate

The present study was approved by the ethical review committee of The Second Affiliated Hospital, School of Medicine, Xi'an Jiaotong University. Written informed consent was obtained from all enrolled patients. The animal experiments were performed following the Guideline to the Management and Use of Laboratory Animals issued by the National Institutes of Health.

Author Contributions

All authors made substantial contributions to conception and design, acquisition of data, or analysis and interpretation of data; took part in drafting the article or revising it critically for important intellectual content; gave final approval of the version to be published; and agree to be accountable for all aspects of the work.

Funding

No funding was received.

Disclosure

The authors declare that they have no competing interests for this work.

References

1. Bray F, Ferlay J, Soerjomataram I, Siegel RL, Torre LA, Jemal A. Global cancer statistics 2018: GLOBOCAN estimates of incidence and mortality worldwide for 36 cancers in 185 countries. *CA Cancer J Clin*. 2018;68(6):394–424. doi:10.3322/caac.21492
2. Kamran SC, D'Amico AV. Radiation therapy for prostate cancer. *Hematol Oncol Clin North Am*. 2020;34(1):45–69. doi:10.1016/j.hoc.2019.08.017
3. Valeriani M, Marinelli L, Macrini S, et al. Radiotherapy in metastatic castration resistant prostate cancer patients with oligo-progression during abiraterone-enzalutamide treatment: a mono-institutional experience. *Radiat Oncol*. 2019;14(1):205. doi:10.1186/s13014-019-1414-x
4. Yadav S, Kowolik CM, Lin M, et al. SMC1A is associated with radioresistance in prostate cancer and acts by regulating epithelial-mesenchymal transition and cancer stem-like properties. *Mol Carcinog*. 2019;58(1):113–125. doi:10.1002/mc.22913
5. Martens-Uzunova ES, Bottcher R, Croce CM, Jenster G, Visakorpi T, Calin GA. Long noncoding RNA in prostate, bladder, and kidney cancer. *Eur Urol*. 2014;65(6):1140–1151. doi:10.1016/j.eururo.2013.12.003
6. Ponting CP, Oliver PL, Reik W. Evolution and functions of long noncoding RNAs. *Cell*. 2009;136(4):629–641. doi:10.1016/j.cell.2009.02.006
7. Misawa A, Takayama K, Urano T, Inoue S. Androgen-induced long noncoding RNA (lncRNA) SOCS2-AS1 promotes cell growth and inhibits apoptosis in prostate cancer cells. *J Biol Chem*. 2016;291(34):17861–17880. doi:10.1074/jbc.M116.718536
8. Fotouhi Ghiam A, Taeb S, Huang X, et al. Long non-coding RNA urothelial carcinoma associated 1 (UCA1) mediates radiation response in prostate cancer. *Oncotarget*. 2017;8(3):4668–4689. doi:10.18632/oncotarget.13576
9. Chen C, Wang K, Wang Q, Wang X. LncRNA HULC mediates radioresistance via autophagy in prostate cancer cells. *Braz J Med Biol Res*. 2018;51(6):e7080. doi:10.1590/1414-431x20187080
10. Yu X, Li Z. Long non-coding RNA growth arrest-specific transcript 5 in tumor biology. *Oncol Lett*. 2015;10(4):1953–1958. doi:10.3892/ol.2015.3553
11. Yacqub-Usman K, Pickard MR, Williams GT. Reciprocal regulation of GAS5 lncRNA levels and mTOR inhibitor action in prostate cancer cells. *Prostate*. 2015;75(7):693–705. doi:10.1002/pros.22952
12. Xie X, Dai J, Huang X, Fang C, He W. MicroRNA-145 inhibits proliferation and induces apoptosis in human prostate carcinoma by upregulating long non-coding RNA GAS5. *Oncol Lett*. 2019;18(2):1043–1048. doi:10.3892/ol.2019.10419
13. Yang J, Hao T, Sun J, Wei P, Zhang H. Long noncoding RNA GAS5 modulates alpha-Solanine-induced radiosensitivity by negatively regulating miR-18a in human prostate cancer cells. *Biomed Pharmacother*. 2019;112:108656. doi:10.1016/j.biopha.2019.108656
14. Hammond SM. An overview of microRNAs. *Adv Drug Deliv Rev*. 2015;87:3–14. doi:10.1016/j.addr.2015.05.001
15. Wei D, Yu G, Zhao Y. MicroRNA-30a-3p inhibits the progression of lung cancer via the PI3K/AKT by targeting DNA methyltransferase 3a. *Onco Targets Ther*. 2019;12:7015–7024. doi:10.2147/OTT.S213583
16. Daniel R, Wu Q, Williams V, Clark G, Guruli G, Zehner Z. A panel of MicroRNAs as diagnostic biomarkers for the identification of prostate cancer. *Int J Mol Sci*. 2017;18:6. doi:10.3390/ijms18061281
17. Duan XM, Liu XN, Li YX, et al. MicroRNA-498 promotes proliferation, migration, and invasion of prostate cancer cells and decreases radiation sensitivity by targeting PTEN. *Kaohsiung J Med Sci*. 2019;35(11):659–671. doi:10.1002/kjm2.12108
18. Wang F, Mao A, Tang J, et al. microRNA-16-5p enhances radiosensitivity through modulating Cyclin D1/E1-pRb-E2F1 pathway in prostate cancer cells. *J Cell Physiol*. 2019;234(8):13182–13190. doi:10.1002/jcp.27989
19. Hudcova K, Trnkova L, Kejnovska I, et al. Novel biophysical determination of miRNAs related to prostate and head and neck cancers. *Eur Biophys J*. 2015;44(3):131–138. doi:10.1007/s00249-015-1008-y
20. Ye F, Tang H, Liu Q, et al. miR-200b as a prognostic factor in breast cancer targets multiple members of RAB family. *J Transl Med*. 2014;12:17. doi:10.1186/1479-5876-12-17
21. Ge J, Chen Q, Liu B, Wang L, Zhang S, Ji B. Knockdown of Rab21 inhibits proliferation and induces apoptosis in human glioma cells. *Cell Mol Biol Lett*. 2017;22:30. doi:10.1186/s11658-017-0062-0
22. Hognas G, Tuomi S, Veltel S, et al. Cytokinesis failure due to derailed integrin traffic induces aneuploidy and oncogenic transformation in vitro and in vivo. *Oncogene*. 2012;31(31):3597–3606. doi:10.1038/onc.2011.527
23. Edge SB, Compton CC. The American Joint Committee on Cancer: the 7th edition of the AJCC cancer staging manual and the future of TNM. *Ann Surg Oncol*. 2010;17(6):1471–1474. doi:10.1245/s10434-010-0985-4
24. Livak KJ, Schmittgen TD. Analysis of relative gene expression data using real-time quantitative PCR and the 2(-Delta Delta C(T)) method. *Methods*. 2001;25(4):402–408. doi:10.1006/meth.2001.1262
25. Taylor SC, Berkelman T, Yadav G, Hammond M. A defined methodology for reliable quantification of Western blot data. *Mol Biotechnol*. 2013;55(3):217–226. doi:10.1007/s12033-013-9672-6
26. Naito S, von Eschenbach AC, Giavazzi R, Fidler IJ. Growth and metastasis of tumor cells isolated from a human renal cell carcinoma implanted into different organs of nude mice. *Cancer Res*. 1986;46(8):4109–4115.
27. Center MM, Jemal A, Lortet-Tieulent J, et al. International variation in prostate cancer incidence and mortality rates. *Eur Urol*. 2012;61(6):1079–1092. doi:10.1016/j.eururo.2012.02.054
28. Mottet N, Bellmunt J, Bolla M, et al. EAU-ESTRO-SIOG guidelines on prostate cancer. Part 1: screening, diagnosis, and local treatment with curative intent. *Eur Urol*. 2017;71(4):618–629. doi:10.1016/j.eururo.2016.08.003

29. Wang W, Liu M, Guan Y, Wu Q. Hypoxia-responsive Mir-301a and Mir-301b promote radioresistance of prostate cancer cells via down-regulating NDRG2. *Med Sci Monit*. 2016;22:(2126–2132. doi:10.12659/MSM.896832
30. Li CH, Chen Y. Insight into the role of long noncoding RNA in cancer development and progression. *Int Rev Cell Mol Biol*. 2016;326:(33–65.
31. Mitobe Y, Takayama KI, Horie-Inoue K, Inoue S. Prostate cancer-associated lncRNAs. *Cancer Lett*. 2018;418:(159–166. doi:10.1016/j.canlet.2018.01.012
32. Lyu K, Xu Y, Yue H, et al. Long noncoding RNA GAS5 acts as a tumor suppressor in laryngeal squamous cell carcinoma via miR-21. *Cancer Manag Res*. 2019;11:(8487–8498. doi:10.2147/CMAR.S213690
33. Li G, Cai Y, Wang C, Huang M, Chen J. LncRNA GAS5 regulates the proliferation, migration, invasion and apoptosis of brain glioma cells through targeting GSTM3 expression. The effect of LncRNA GAS5 on glioma cells. *J Neurooncol*. 2019;143(3):525–536. doi:10.1007/s11060-019-03185-0
34. Yang W, Xu X, Hong L, Wang Q, Huang J, Jiang L. Upregulation of lncRNA GAS5 inhibits the growth and metastasis of cervical cancer cells. *J Cell Physiol*. 2019;234(12):23571–23580. doi:10.1002/jcp.28926
35. Wang C, Ke S, Li M, Lin C, Liu X, Pan Q. Downregulation of LncRNA GAS5 promotes liver cancer proliferation and drug resistance by decreasing PTEN expression. *Mol Genet Genomics*. 2019.
36. Long X, Song K, Hu H, et al. Long non-coding RNA GAS5 inhibits DDP-resistance and tumor progression of epithelial ovarian cancer via GAS5-E2F4-PARP1-MAPK axis. *J Exp Clin Cancer Res*. 2019;38(1):345. doi:10.1186/s13046-019-1329-2
37. Gao J, Liu L, Li G, et al. LncRNA GAS5 confers the radio sensitivity of cervical cancer cells via regulating miR-106b/IER3 axis. *Int J Biol Macromol*. 2019;126:(994–1001. doi:10.1016/j.ijbiomac.2018.12.176
38. Xue Y, Ni T, Jiang Y, Li Y. Long noncoding RNA GAS5 inhibits tumorigenesis and enhances radiosensitivity by suppressing mir-135b expression in non-small cell lung cancer. *Oncol Res*. 2017;25 (8):1305–1316. doi:10.3727/096504017X14850182723737
39. Su P, Mu S, Wang Z. Long noncoding RNA SNHG16 promotes osteosarcoma cells migration and invasion via sponging miRNA-340. *DNA Cell Biol*. 2019;38(2):170–175. doi:10.1089/dna.2018.4424
40. Peng W, Deng W, Zhang J, Pei G, Rong Q, Zhu S. Long noncoding RNA ANCR suppresses bone formation of periodontal ligament stem cells via sponging miRNA-758. *Biochem Biophys Res Commun*. 2018;503(2):815–821. doi:10.1016/j.bbrc.2018.06.081
41. Zhao W, Sun Q, Yu Z, et al. MiR-320a-3p/ELF3 axis regulates cell metastasis and invasion in non-small cell lung cancer via PI3K/Akt pathway. *Gene*. 2018;670:(31–37. doi:10.1016/j.gene.2018.05.100
42. Mundalil Vasu M, Anitha A, Takahashi T, et al. Fluoxetine increases the expression of miR-572 and miR-663a in human neuroblastoma cell lines. *PLoS One*. 2016;11(10):e0164425. doi:10.1371/journal.pone.0164425
43. Wang W, Zhao L, Wei X, et al. MicroRNA-320a promotes 5-FU resistance in human pancreatic cancer cells. *Sci Rep*. 2016;6:(27641. doi:10.1038/srep27641
44. Steber HS, Gallante C, O'Brien S, Chiu PL, Mangone M. The C. elegans 3′ UTRome v2 resource for studying mRNA cleavage and polyadenylation, 3′-UTR biology, and miRNA targeting. *Genome Res*. 2019;29(12):2104–2116. doi:10.1101/gr.254839.119
45. Wang H, Huang W, Yu X, et al. Two prostate cancer-associated polymorphisms in the 3′UTR of IGF1R influences prostate cancer susceptibility by affecting miRNA binding. *Oncol Rep*. 2019;41 (1):512–524. doi:10.3892/or.2018.6810